Eur Biophys J (2005) 34: 255–261
DOI 10.1007/s00249-004-0447-7

ARTICLE

Martial Balland · Alain Richert · François Gallet

# The dissipative contribution of myosin II in the cytoskeleton dynamics of myoblasts

Received: 6 August 2004 / Revised: 6 November 2004 / Accepted: 11 November 2004 / Published online: 18 December 2004


**Abstract** We have determined the microrheological response of the actin meshwork for individual cells. We applied oscillating forces with an optical tweezer to a micrometric bead specifically bound to the actin meshwork of C2 myoblasts, and measured the amplitude and phase shift of the induced cell deformation. For a non-perturbed single cell, we have shown that the elastic and loss moduli G′ and G″ behave as power laws $f^{\alpha}$ and $f^{\beta}$ of the frequency $f$ ($0.01 < f < 50$ Hz), $\alpha$ and $\beta$ being in the range 0.15–0.35. This demonstrates that the dissipation mechanisms in a single cell involve a broad and continuous distribution of relaxation times. After adding blebbistatin, an inhibitor of myosin II activity, the exponent of G′ decreases to about 0.10, and G″ becomes roughly constant for $0.01 < f < 10$ Hz. The actin meshwork appears less rigid and less dissipative than in the control experiment. This is consistent with an inhibition of ATPase and reduction of the gliding mobility of myosin II on actin filaments. In this frequency range, the actomyosin activity appears as an essential mechanism allowing the cell to adapt to an external mechanical stress.

**Keywords** Actin meshwork viscoelasticity · Myosin · Microrheology · Optical tweezers · Blebbistatin

M. Balland · A. Richert · F. Gallet
Laboratoire de Biorhéologie et Hydrodynamique Physico-chimique, UMR 7057 associée au CNRS et à l'Université Paris 7, Case courrier 7056—2, place Jussieu, 75251 Paris Cedex 05, France

M. Balland · A. Richert · F. Gallet (✉)
Fédération de Recherche "Matière et Systèmes Complexes" FR 2438, associée au CNRS et à l'Université Paris 7, Case courrier 7056—2, place Jussieu, 75251 Paris Cedex 05, France
E-mail: frgallet@ccr.jussieu.fr
Tel.: +33-1-44277782
Fax: +33-1-44274335

## Introduction

The cytoskeleton plays a crucial role in the cell's mechanical behaviour. It can withstand large stresses, and enables the cell to resist external stresses and to maintain its structural integrity. Also, the cytoskeleton's dynamical properties and interactions with associated proteins, especially molecular motors, makes it an essential regulatory element in many functions such as cell adhesion, migration and division. Moreover, the cytoskeleton filaments can both transmit mechanical efforts and carry chemical charges from the cell's periphery towards the inner cell parts and nucleus, and thus participate in several mechanotransduction processes (Janmey 1998). This explains why the mechanical properties of the cytoskeletal network are the subject of many experimental studies. These works have been made possible by the development of numerous quantitative micromanipulation techniques, such as micropipettes (Sato et al. 1996), cell poking (Petersen et al. 1982), shear flow cytometry (Dewey et al. 1981; Barbee et al. 1994), atomic force microscopy (AFM) (Rotsch et al. 1997; Sato et al. 2000; Alcaraz et al. 2003), microplates (Thoumine and Ott 1997; Caille et al. 2002), optical tweezers (Laurent et al. 2002) and stretchers (Guck et al. 2001), magnetic tweezers (Bausch et al. 1999; Wilhelm et al. 2003) and twisters (Laurent et al. 2002; Fabry et al. 2001) and particle tracking (Tseng et al. 2002). These techniques are complementary, in the sense that they probe the behaviour of the intracellular medium at different length scales and time scales, and implement stresses and strains of different nature and having different orders of magnitude. Although the microtubule and intermediate filament networks are known to participate in the response of the cellular medium(Janmey et al. 1991; Caspi et al. 2002), many results focus on the mechanical behaviour of the actin meshwork, which is made possible by specifically directing the probe towards actin filaments.

As a consequense of the diversity of the techniques used, one does not expect the results of the various experiments to match exactly, but some general features may be drawn: (1) the apparent elastic modulus that was measured seems to decrease with the probe size (Maksym et al. 2000), and its dispersion reflects the heterogeneous density of the actin meshwork inside the cell (Wilhelm et al. 2003; Yamada et al. 2000); (2) dissipation phenomena inside the cell cannot be assigned to a single time relaxation, nor to a finite number of time relaxations. Practically, this means that it is not possible to accurately model the cell's mechanical behaviour by associating several springs and dashpots, respectively accounting for elastic restoring forces and viscous damping. In other words, a simple picture of the cellular medium as a Maxwell viscoelastic liquid or a Kelvin–Voigt solid, or any finite combination of them, is not realistic. This conclusion is supported by several microrheological experiments. Fabry et al. (2001) have measured the complex viscoelastic response $G(f) = G'(f) + iG''(f)$ of human airway smooth muscle cells submitted to an oscillating force at frequency $f$. They showed that, on average, both the storage ($G'$) and loss ($G''$) moduli behave as the same power law $f^{\alpha}$ of the frequency, in the range $0.01 < f < 100$ Hz. The exponent $\alpha$ is found between 0.15 and 0.30. The same kind of power-law behaviour was observed in lung epithelial cells by an oscillating indentation experiment with AFM (Alcaraz et al. 2003). Moreover, the free motion of particles microinjected in a cell's cytoplasm exhibits non-standard sub-diffusive or super-diffusive behaviour (Tseng et al. 2002) at different time scales, which cannot be interpreted within a classical viscous fluid picture. These results tend to show that the dissipation processes inside the cell involve a continuous distribution of relaxation times. It has also been noted that the viscoelastic response of cells is on average similar to that of soft glassy materials (Sollich et al. 1997; Sollich 1998), but the elementary mechanisms possibly explaining this analogy have not been identified.

At this stage, several questions arise. Prior to any interpretation of the dissipative mechanisms in the actin meshwork, a precise knowledge of the viscoelastic response of a single cell is required. The power laws $G'$, $G'' \propto f^{\alpha}$ were established by analyzing the average response of several cells, and this averaging may mask some individual features. It has been reported that power laws remain valid on a cell-by-cell basis (Fabry et al. 2003; Puig-de-Morales et al. 2004; Lenormand et al. 2004), but no demonstrative data on single cells have ever been published. Thus, this point still needs to be carefully investigated.

Another key issue is to understand the origins of the dissipation inside the cell. Considering a continuous range of relaxation times, it is crucial to identify the respective contribution to the mechanical response of the different dissipative mechanisms, such as actin polymerisation and depolymerisation, filament cross-linking, and molecular motor activity. This can be done by specifically enhancing or inhibiting one of these processes, and measuring how the meshwork's viscoelastic response is affected. Concerning the dynamics of actin filaments, it has already been shown that the depolymerising action of cytochalasin D makes the meshwork softer and more fluid (Fabry et al. 2001), and prevents the cell from reorganising over a large time scale ($> 15$ min) after uniaxial stretching (Thoumine and Ott 1997). Similar effects were observed with latrunculin, an actin-disrupting agent (Wilhelm et al. 2003; Yamada et al. 2000). On the other hand, the role played by molecular motors is far from being fully elucidated. Recent studies have shown that the viscoelastic coefficient $G(f) = G' + iG''$ of in vitro actin gels also scales with frequency $f$ as a power law $f^{\alpha}$, where $\alpha$ is close to 0.75 in the passive state (Amblard et al. 1996; Palmer et al. 1999), and increases to 0.87 when myosin is ATP-activated (Le Goff et al. 2002). This indicates that, in vitro, the activity of the actomyosin complex enhances the longitudinal filament fluctuations, and makes the gel response closer to that of a purely viscous fluid. In living cells, adding myosin inhibitors changes the mechanical answer to a stress under static conditions (An et al. 2002). However, to our knowledge, no study has yet been reported concerning the frequency-dependent microrheological response of the actin meshwork in living cells, while specifically blocking the actomyosin complex activity in a controlled way.

The present work brings two distinct contributions to the discussion above. In this experimental study, we used an optical tweezer to apply controlled mechanical forces to the actin meshwork in C2 myoblasts, via silica microbeads bound to transmembrane integrins. Firstly, for each individual cell, the dynamical viscoelastic response $G(f) = G'(f) + iG''(f)$ was measured as a function of frequency $f$, in the range $0.05 < f < 50$ Hz. We show that power laws $G'$, $G'' \propto f^{\alpha}$ accurately describe the mechanical behaviour of individual cells. Secondly, we used blebbistatin to specifically block the myosin II activity inside the living cell (Straight et al. 2003, Kovacs et al. 2004). Blebbistatin has been shown to inhibit the adenosine triphosphatase (ATPase) and the gliding mobility of myosin II in human platelets, but it does not modify the activity of myosin light-chain kinase. Comparing the individual mechanical response of control cells and of cells treated with blebbistatin, we show that their behaviours are noticeably different. The elastic and loss moduli $G'(f)$ and $G''(f)$ of treated cells are both smaller than for control cells. Moreover, for treated cells, $G'(f)$ still exhibits a power law $f^{\alpha'}$, but with $\alpha'$ of the order of 0.1, smaller than for control cells. At the same time, the loss modulus $G''(f)$ of the treated cells remains nearly constant in the range 0.05–10 Hz, and increases rapidly for $f > 10$ Hz. Thus, inhibiting the actomyosin complex by blebbistatin simultaneously induces a decrease in rigidity and a more elastic behaviour of the actin meshwork. This result shows that the myosin activity makes the meshwork more rigid and

more dissipative, especially in the range of time scales larger than 100 ms.

## Methods

The muscular cell line C2 (kindly provided by M. Lambert and R.M. Mège, INSERM U440, Institut du Fer à Moulin, Paris) was maintained in a stock callus culture in Dulbecco's Modified Essential Medium with 4.5 g/l glucose, 200 mM glutamine, 20% heat-inactivated FCS and penicillin–streptomycin (penicillin = 10,000 U/ml, streptomycin = 10 mg/ml). Cells were grown at 37°C under a humidified 5% $CO_2$ atmosphere. Every 3 days, just before confluent state, cells were subcultivated in a volume of 5 ml of fresh medium. The day before experiments, cells were detached (1% trypsin and 1 mM EDTA) and were grown on 22×22-mm glass coverslips coated with 5 μg/ml fibronectin.

To probe the dynamic properties of the actin cytoskeleton, carboxylated silica microbeads (3.47-μm diameter, Bangs Laboratories Inc., IN, USA) were specifically bound to integrin and used as handles to apply mechanical stress to the cell with an optical trap. The specific binding was achieved by coating the beads with arginine–glycine–aspartic tripeptide (RGD), according to the manufacturer's procedure (Telios pharmaceuticals, CA, USA). To prevent non-specific binding, coated beads were incubated in a serum-free culture medium supplemented with 1% BSA at 37°C. Thirty minutes before starting the experiment, the bead suspension (50 μg/ml) was added to the cells at 37°C, in order to bind between 1 and 5 beads to each cell (see Fig. 1a). Unbound beads were washed away with serum-free culture medium 1% BSA. A closed experimental chamber was made by sealing the coverslip to a microscope slide, separated by a plastic film spacer (80 to 150 μm thick). This chamber was mounted on a piezoelectric stage (model P-780 Polytec PI), allowing constant or variable displacements, in the range 0–100 Hz (maximum excursion 80 μm). The whole set-up was placed on the plate of an inverted microscope (Leica DMIRB). All measurements were performed in a 37°C thermalisation box (Life Imaging services, Switzerland).

As a blocker of the actomyosin complex, we used a molecular tool that specifically targets myosin II. It has been shown that blebbistatin exclusively acts on myosin II, inhibiting ATPase and gliding motility of myosin in human platelets (Straight et al. 2003). We prepared a 75-mM stock solution in DMSO of (±) blebbistatin—a racemic mixture of both enantiomers—(Fisher Bioblock Scientific, Illkirch, France). We checked the concentration by using the extinction coefficient 7,400 $M^{-1}$ $cm^{-1}$ at 422 nm (Straight et al. 2003). The stock solution was diluted 1,000 times in the culture medium in which the cells were grown. At this concentration (75 μM), the relative ATPase activity and the gliding filament velocity are reduced to 5 and 20% of their initial value, respectively (Straight et al. 2003).

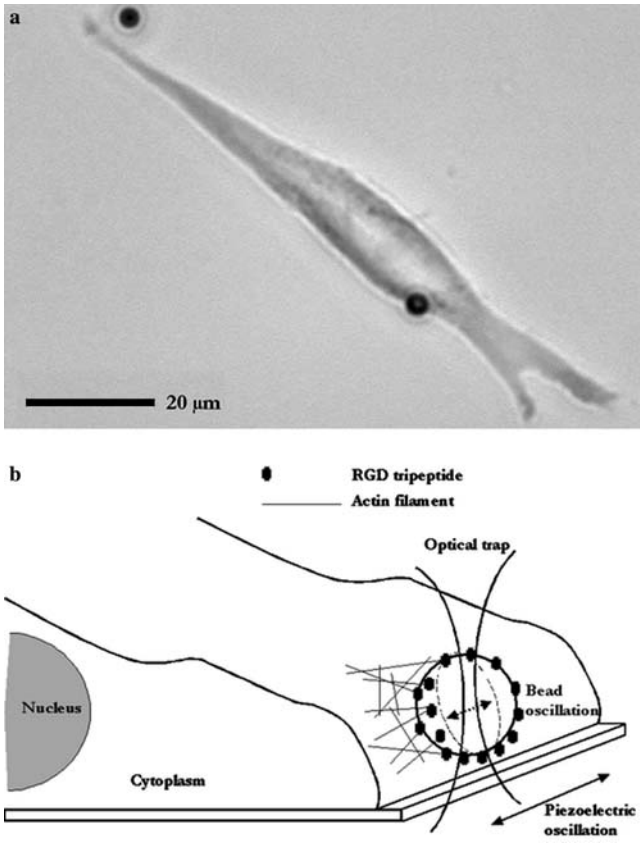


**Fig. 1** **a** View of a C2 myoblast grown on a fibronectin-coated coverslip. A 3.47-μm-silica bead, coated with RGD peptide, specifically binds to the transmembrane integrins and thus can be used as a handle to apply calibrated forces to the actin network. **b** Principle of the microrheology experiment: the piezoelectric stage makes the chamber oscillate at frequency $f$, while the bead is trapped in the optical tweezer. The bead position $x_b$ and the stage position $x_c$ are recorded with a fast camera. The viscoelastic modulus $G(f)$ is deduced from the complex ratio of the force exerted by the trap $F(x_b)$ over the cell deformation $x_c - x_b$

The experiments were performed with a dynamic optical tweezers set-up. The set-up used for optical trapping has been described in detail elsewhere (Lenormand et al. 2001), and the principle is schematically represented in Fig. 1b. Briefly, the electric-field gradient created by an infrared laser beam ($P_{max} = 600$ mW) strongly focused through the oil immersion objective of the microscope (×100, NA = 1.25) generates a trapping force on a dielectric micrometric particle, for instance a silica or a latex microbead. In the absence of any external force, the bead is at equilibrium at the trap centre. The trapping force depends on the bead-trap distance $\Delta x$, on the laser beam total power, and also on the size and shape of the trapped object. Its precise characterisation requires an independent calibration. A widely used calibration method consists in trapping a free bead and submitting it to a counterflow of known velocity $v$. At the new equilibrium position $\Delta x$, the trapping force $F(\Delta x)$ equilibrates the viscous drag force, given by the Stokes formula $F = 6\pi\eta Rv$, $R$ denoting the

particle radius and $\eta$ the viscosity of the surrounding liquid.

For a cell, the force-deformation relationship is obtained by applying to the experimental chamber a sinusoïdal displacement $x_c$ at frequency $f$, and simultaneously trapping a bead bound to the cell membrane in the optical trap at a fixed position. At any time, the force exerted on the bead is related to the bead-trap distance $\Delta x = x_b$, while the cellular deformation is measured by the relative displacement $x_c - x_b$ between the chamber and the bead. Lateral bead motion $x_b$ and chamber motion $x_c$ are detected by using a fast camera (Kodak SR500). A Labview program was written to synchronously generate a sequence of successive sinusoidal trains at different frequencies, which control the piezoelectric ceramic motion, and a sequence of pulses, which trigger the image acquisition. This ensures that the phase shift between the applied force and the measured deformation is accurately determined. Typically, the amplitude of the stage motion is 1.55 μm, its frequency $f$ is swept from 0.05 to 41.5 Hz, and about 5–20 images are recorded during each period. The images, sampled with a 16 bits video-acquisition card (IMAQ PCI/PXI-1407, exposure time 2 ms), were analysed using a pattern-matching algorithm (Imaq vision Builder, Texas Instrument NI, USA) in which subpixel arithmetic allows a spatial resolution of 20 nm. To avoid a possible actin meshwork remodelling at the bead periphery on a large time scale, or a slow drift of the bead on the cell surface, the measurements' total duration on the same single cell never exceeds 2.5 min.

To analyse the optical tweezers' cytometry data, we need a mechanical model. We consider the spherical bead as a probe of the viscoelastic properties of the actin cytoskeleton. The intracellular medium is assumed to be semi-infinite, incompressible, and characterised in the zero frequency limit either by its Young elastic modulus E (purely elastic solid case) or its viscosity $\eta$ (purely viscous fluid case). As shown in a previous paper (Laurent et al. 2002), we have established, in the small deformation regime, the linear relationships between the relative bead-cell displacement $x = x_c - x_b$ and the restoring elastic force F exerted by the stressed medium, for different geometric configurations. In this model, we took into account the angle of immersion $\theta$ ($0 < \theta < 180°$) of the bead into the cell (this angle can be measured for each cell by video-microscopy). In current experimental situations, it lies between 20° and 50°. We have shown that the relation between $x$ and F can be written as either $F = 2\pi RE\, h(\theta)\, x$ (purely elastic medium) or $F = 6\pi R\eta\, h'(\theta)\, d\,x/d\,t$ (purely newtonian viscous liquid). The two functions $h(\theta)$ and $h'(\theta)$ are geometric factors depending on the angle $\theta$ of immersion of the bead into the cell. For instance, when the force F is applied tangentially to the cell membrane, we have calculated that $h(\theta) = [9/(4\ \sin\theta) + 3\ \cos\theta/(2\ \sin^3\theta)]^{-1}$. Here, we generalise the above description for a complex viscoelastic medium as follows: assuming that the bead is submitted to an oscillating force $F = F_0 \exp(2i\pi ft)$ at frequency $f$, the displacement induced may be written as $x = x_0 \exp(2i\pi ft)$, and the static relationship $F = 2\pi RE\, h(\theta)\, x$ is generalised into $F_0 = 2\pi RG(f)\, h(\theta)\, x_0$. Here, $G(f) = G'(f) + i\, G''(f)$ represents the frequency-dependant complex elastic modulus, split into its real part G′ (storage modulus) and G″ (loss modulus). G′ and G″ are, respectively, the in-phase and out-of-phase answers to an applied specific stress of amplitude unity.

In a typical run, we measure for each single cell the amplitude of the oscillating force applied to the cell's actin cytoskeleton via the trapped bead, and the induced cell deformation, and also their relative phase shift. From this, we deduce the complex elastic modulus G($f$) for each frequency of the sequence.

## Results

### Control C2 cells in culture

We have plotted for each individual cell both the elastic modulus G′($f$) and the loss modulus G″($f$) as a function of frequency $f$, in the range 0.05–50 Hz. An example of such a plot on logarithmic scale is shown in the inset of Fig. 2. For this cell, G′ and G″ behave as power laws of the frequency, over three decades, with respective exponents $\alpha = 0.29$ and $\beta = 0.33$ This power-law behaviour is found to be valid for each individual cell; the exponents $\alpha$ and $\beta$ show slight variations from one cell to the other, but they remain in the following ranges:

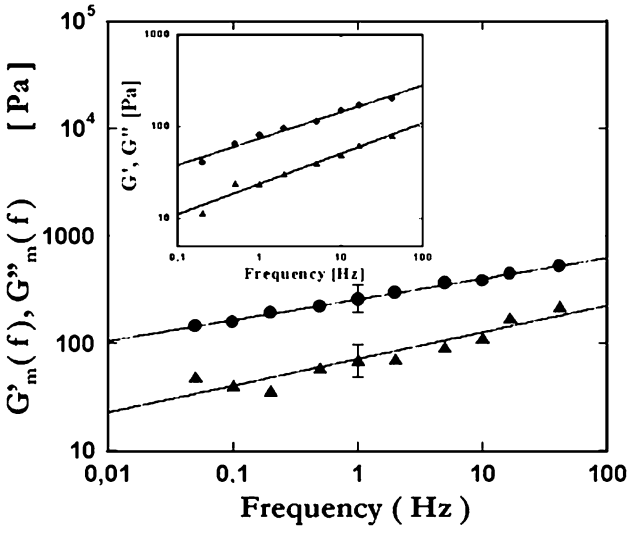


**Fig. 2** Plots of the elastic modulus G′ (*circles*) and loss modulus G″ (*triangles*) of the cytoskeletal network versus frequency $f$ for unperturbed C2 cells. The *inset* reports the values of G′ and G″ measured for a single typical cell. The main plot represents the geometrical averages $G'_m$ and $G''_m$ ($n = 21$cells). The best power-law fits $G' \propto f^{\alpha}$ and $G'' \propto f^{\beta}$ are also drawn. One finds $\alpha = 0.29$ and $\beta = 0.33$ for the single cell, $\alpha_m = 0.19$ and $\beta_m = 0.25$ for the average curves. This shows that G′($f$) and G″($f$) are accurately represented by power laws, with $\alpha \approx \beta$, and that the dissipation mechanisms in a single cell involve a continuous distribution of relaxation times

$0.1 < \alpha < 0.4$ and $0.1 < \beta < 0.5$. Their average values over 21 cells are $<\alpha> = 0.20 \pm 0.02$ and $<\beta> = 0.29 \pm 0.04$. For each cell, the exponents $\alpha$ and $\beta$ generally remain close together, although most of the time $\beta$ is found slightly larger than $\alpha$: on average, $<\beta\text{-}\alpha> = 0.09 \pm 0.03$. The main graph in Fig. 2 represents the geometrical averages $G'_m(f) = [\Pi\ G'_i(f)]^{1/21}$ and $G''_m = [\Pi\ G''_i(f)]^{1/21}$ over the same 21 cells, plotted versus frequency. $G'_m$ and $G''_m$ also exhibit a power law versus frequency, with respective exponents $\alpha_m = 0.19$ and $\beta_m = 0.25$. The magnitudes of $G'_m$ and $G''_m$ may be characterised by their geometrical averages and standard errors at $f = 1$ Hz: $G'_m$ (1 Hz) $= 260 \pm 80$ Pa and $G''_m$ (1 Hz) $= 70 \pm 25$ Pa.

Such a power-law behaviour is not unusual. In a magnetic twisting experiment, Fabry et al. (Fabry et al. 2001) have already observed that the values of $G'$ and $G''$, averaged over a large number of cells, vary like $f^{\alpha}$, the exponent $\alpha \cong 0.15$–$0.30$ being the same for $G'$ and $G''$ in a first approximation. In another experiment (Lau et al. 2003), the time-fluctuation spectrum of endogenous tracers embedded in the cytoplasm and the two-point spatial correlation spectrum were also found to behave as power laws. In the same way, creep experiments on single cells (Desprat et al. 2005) exhibit a power-law creep response, with similar exponents $\alpha \cong 0.15$–$0.30$. The significantly new result brought by our experiment-and by the creep experiment-is that this behaviour is clearly stated not only for an ensemble average, but also for individual cells. Indeed, due to the dispersion from one cell to the other, an ensemble average generally smooths individual features, and the average response may not reflect the different individual responses. This does not occur in a cell-by-cell analysis. The fact that the mechanical response of each cell is correctly represented by power laws can be directly related to the dissipation mechanisms in the cytoskeleton. In a discrete elements model associating springs and dashpots, the mechanical response of a cell would reduce to a finite sum of exponential curves and there would exist a finite number of relaxation times in the system (Thoumine and Ott 1997; Bausch et al. 1999). In contrast, a wide range of dissipation mechanisms, and thus a continuous distribution of relaxation time, lead to other types of responses, like power laws. This is not surprising because in a living cell various mechanisms contribute to cytoskeleton remodelling: dynamical polymerisation of actin and treadmilling, filament cross-linking and actomyosin complex activity, each of them corresponding to specific spatial and temporal scales. Of course, modelling the mechanical response by enough discrete elements (of the order of six) may fit the single cell data as well. Besides the fact that this requires more parameters than a simple power-law fit, a small number of relaxation times is hardly compatible with the above picture, which involves a wide range of dissipation phenomena. Thus, the present data, together with other mechanical characterisations (Fabry et al. 2003; Lau et al. 2003; Puig-de-Morales et al. 2004; Lenormand et al. 2004; Desprat et al. 2005), rule out a possible modelling in terms of discrete elements, and demonstrate that the dissipation mechanisms involve a continuous range of relaxation times.

## C2 cells with blebbistatin added

The microrheological response of cells treated with blebbistatin is significantly different from that of unperturbed cells. The inset of Fig. 3 shows a typical plot of $G'(f)$ and $G''(f)$ for an individual cell with blebbistatin added. The elastic modulus $G'(f)$ still behaves like $f^{\alpha'}$, but the exponent $\alpha' = 0.11$ is smaller than the exponent $\alpha \cong 0.20$ measured for unperturbed cells. On the other hand, the loss modulus $G''$ remains almost constant in the frequency range 0.1–10 Hz, and rapidly increases with $f$ when $f > 10$ Hz. The same behaviour is observed in a sample of 15 C2 cells. The average value of $\alpha'$ over these cells is $<\alpha'> = 0.07 \pm 0.02$, and one finds the same two regimes for $G''(f)$. This single cell behaviour identically reproduces the geometrical averages $G'_m(f)$ of $G'(f)$ and $G''_m(f)$ of $G''(f)$, calculated over 15 cells (see Fig. 3). $G'_m(f)$ is accurately fitted by a power law $f^{\alpha'_m}$, with $\alpha'_m = 0.06$, significantly smaller than the exponent $\alpha_m = 0.19$ measured for unperturbed cells. Similarly, $G''_m(f)$ remains constant in the range 0.01–10 Hz, before rapidly increasing above 10 Hz. The magnitudes of $G'_m$ and $G''_m$ at $f = 1$ Hz are $G'_m$ (1 Hz) $= 57 \pm 22$ Pa and $G''_m$ (1 Hz) $= 13 \pm 6$ Pa, respec-

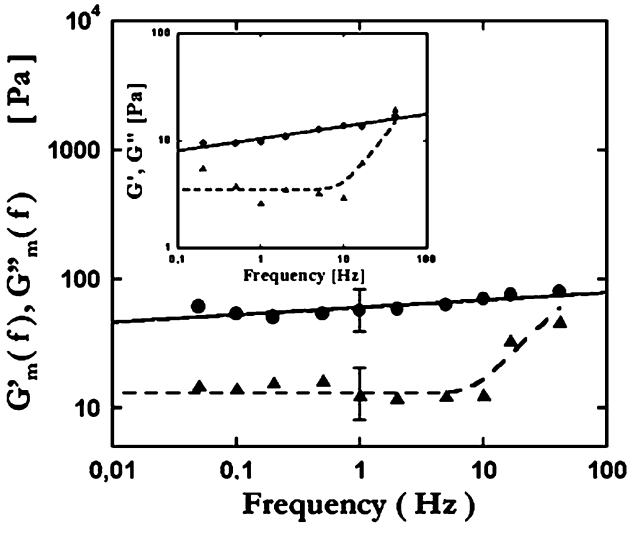


**Fig. 3** Same plots of $G'$ and $G''$ as in Fig. 2, for cells treated with blebbistatin, which inhibits the activity of the actomyosin complex. Both for an individual cell (*inset*) and for the ensemble average (main plot, $n = 15$ cells), the exponent of the fit $G' \propto f^{\alpha'}$ is reduced, respectively, to $\alpha' = 0.11$ and $\alpha'_m = 0.06$. The loss modulus $G''$ is roughly independent of the frequency in the range 0.05–10 Hz, and rapidly increases above 10 Hz (*dashed lines* are guides for the eye). The magnitudes of $G'$ and $G''$ at $f = 1$ Hz are about five times lower than for control cells. This indicates that inhibiting the myosin motor activity by blebbistatin makes the network less dissipative, and simultaneously less rigid

tively. Both of these values are about five times lower than those measured for unperturbed cells. These sharp differences between control cells and cells treated with blebbistatin are a clear signature of actomyosin complex activity. A detailed interpretation of these results is proposed in the following discussion.

## Discussion

Let us first comment on the power-law microrheological response of C2 cells in control experiments. A behaviour where both $G'(f)$ and $G''(f)$ vary like $f^{\alpha}$ is rather common in complex viscoelastic media, like micellar and polymer solutions, or colloidal suspensions, and reflects the wide distribution of relaxation times in these non-active systems. In this case, the exponent $\alpha$ represents the degree of fluidity of the system: $\alpha$ varies from 0 for a pure elastic solid to 1 for a pure viscous fluid. In a very crude picture, which does not take into account the biological activity, the intra-cellular medium can be compared to such a complex medium. This description seems adequate in the case of dilute in vitro actin solutions (Amblard et al. 1996; Palmer et al. 1999), where one measured $\alpha = 0.75$. Of course, the dynamics inside a living cell must include the out-of-equilibrium character of the biochemical activity. In a more elaborated approach (Fabry et al. 2001), the cytoplasm was compared to a "soft glassy material", a class of disordered out-of-equilibrium systems, including foams, slurries, and granular materials, in which the dissipation is controlled by active, non-viscous mechanisms (Sollich et al. 1997; Sollich 1998). Assuming that the distribution of relaxation times in such a system is a power law, one predicts that both $G'(f)$ and $G''(f)$ behave like $f^{\alpha}$, which is compatible with experimental observations. However, this model is based on very general assumptions, and the link to the microscopic mechanisms regulating the cytoskeleton dynamics is not explicit. Moreover, such a general model cannot predict small deviations from the standard $f^{\alpha}$ law, like the fact that we measure two slightly different exponents for $G'$ and $G''$. More phenomelogical models exist, based on a linear response theory of an active gel, and which take into account the polymerisation/depolymerisation of actin filaments, and the activity of molecular motors (Kruse et al. 2004). After having included the present data, such models are expected to be more appropriate to accurately describe the mechanical response of the cytoskeleton's active meshwork.

Now we turn to the comparison between control cells and blebbistatin-treated cells. Two main features appear: (1) the mechanical response of treated cells is closer to a pure elastic solid, as the exponents of $G'(f)$ and $G''(f)$ decrease when blebbistatin is added (from 0.19 to 0.06 for $G'$ and from 0.25 to about 0 for $G''$, at least in the domain $f < 10$ Hz); (2) control cells are more rigid than treated ones, as both the magnitudes of $G'$ and $G''$ are about five times larger in the first case. This can be understood by analysing the mechanism by which blebbistatin inhibits the actomyosin activity. Blebbistatin was shown to act on myosin II by inhibiting adenosine triphosphatase activity (Straight et al. 2003). Thus, with blebbistatin, ATP is less easily hydrolysed, and remains bound to the myosin head for a longer time than in control conditions. The effect of blebbistatin is not only to decrease the motor activity of the myosin, but furthermore to keep the myosin heads detached from the actin filament for a longer time (Kovacs et al. 2004). Then, one understands that blebbistatin makes the actin meshwork more elastic by preventing the filaments gliding and inhibiting this active dissipation process, and simultaneously less rigid by decreasing the average number of cross-links in the meshwork. This is in quite good agreement with our observations. It is interesting to note that our results are also consistent with the experiments concerning in vitro actin gels with myosin added (Le Goff et al. 2002). In this case, when ATP is depleted, the actomyosin complex passes from the active state to the rigor state, and the exponent $\alpha$ of the power law $|G| \propto f^{\alpha}$ decreases. At the same time, one observes an increase in $|G|$, because ATP depletion causes myosin to remain bound to the actin filaments, increasing the average number of cross-links and thus the rigidity of the meshwork.

Finally, let us briefly comment on the behaviour of $G''$ above 10 Hz. The rapid increase in $G''$ with frequency $f$ suggests that the dissipation in this range may be dominated by a viscous mechanism. Adjusting the $G''$ data above 10 Hz with a viscous damping $G''(f) = 6\pi\eta f$ leads to $\eta \approx 0.07$ Pa.s, a value comparable to the measurements of the intrinsic viscosity of the cytosol (Yamada et al. 2000; Fabry et al. 2001; Wilhelm et al. 2003).

A comparison between the mechanical behaviours of the actin meshwork reported in Figs. 2 and 3 suggests that most of the active dissipative mechanisms are inhibited when blebbistatin is added. Indeed, the elastic modulus $G'$ becomes almost frequency independent, while the loss modulus $G''$ decreases, and meets a pure viscous fluid behaviour at high frequency. This suggests that, in a living cell, the activity of the actomyosin complex is the main source of active dissipation, at least in the frequency range (0.01–50 Hz) investigated. It is largely responsible for the power-law behaviour measured for both $G'(f)$ and $G''(f)$ in control cells. Also, modelling the mechanical contribution of this molecular mechanism could enlight the comparison of the cytoskeletal meshwork with a "soft glassy material", because this model is appropriate to describe out-of-equilibrium systems, in which the stress relaxation is controlled by an active dissipative process.

To conclude, we would like to emphasise that our optical tweezer set-up allows one to determine the microrheological response of the cytoskeletal meshwork in a single cell. For the first time, we discovered that the response of a single myoblast is identical to the ensemble average over several cells. In control experiments, both the elastic modulus $G'(f)$ and the loss modulus $G''(f)$

behave as power laws of the frequency $f$, in the range 0.05–50 Hz. The two exponents are close to 0.25; however, slightly larger for $G''$. Adding blebbistatin, which inhibits the myosin activity, makes the meshwork simultaneously more elastic and less rigid. Our interpretation is that the filament gliding generated by the myosin activity is the main dissipation mechanism in this frequency range. The experimental data, both for control cells and cells treated with blebbistatin, are consistent with the expected behaviour of a soft glassy material, all the more as we have identified the principal mechanism of active dissipation in this out-of-equilibrium system. We are currently expecting quantitative predictions from more phenomenological models, which take into account the detailed mechanisms of the cytoskeletal dynamics, and which should corroborate this general description.

**Acknowledegments** We are grateful to Cécile Sykes and Ewa Paluch for sharing the blebbistatin protocol, and Atef Asnacios, Nicolas Desprat and Jean-François Joanny for helpful discussions. This work was partly supported by grants from the French Ministère de la Recherche (ACI Jeune chercheur), the Université Paris 7 (Bonus Qualité Recherche) and the Centre National de la Recherche Scientifique (bourse de docteur-ingénieur).

## References

Alcaraz J, Buscemi L, Grabulosa M, Trepat X, Fabry B, Farré R, Navajas D (2003) Microrheology of human lung epithelial cells measured by atomic force microscopy. Biophys J 84:2071–2079

Amblard F, Maggs AC, Yurke B, Pargellis AN, Leibler S (1996) Subdiffusion and anomalous local viscoelasticity in actin networks. Phys Rev Lett 77:4470–4473; Erratum Phys Rev Lett 81:1136

An SS, Laudadio RE, Lai J, Rogers RA, Fredberg JJ (2002) Stiffness changes in cultured airway smooth muscle cells. Am J Physiol Cell Physiol 283:C792–C801

Barbee KA, Davies PF, Lal R (1994) Shear stress-induced reorganization of the surface topography of living endothelial cells imaged by atomic force microscopy. Circ Res 74:163–171

Bausch AR, Möller W, Sackmann E (1999) Measurement of local viscoelasticity and forces in living cells by magnetic tweezers. Biophys J 76:573–579

Caille N, Thoumine O, Tardy Y, Meister J-J (2002) Contribution of the nucleus to the mechanical properties of endothelial cells. J Biomech 35:177–187

Caspi A, Granek R, Elbaum M (2002) Diffusion and directed motion in cellular transport. Phys Rev E 66:011916-1; 011916-12

Dewey CF Jr, Bussolari SR, Gimbrone MA Jr, Davies PF (1981) The dynamic response of vascular endothelial cells to fluid shear stress. J Biomech Eng 103:177–188

Desprat N, Richert J, Siméon J, Asnacios A (2005) Creep function of a single living cell. Biophys J Vol 88, March 2005 (In press)

Fabry B, Maksym GN, Butler JP, Glogauer M, Navajas D, Fredberg JJ (2001) Scaling the microrheology of living cells. Phys Rev Lett 87:148102-1;148102-4

Fabry B, Maksym GN, Butler JP, Glogauer M, Navajas D, Taback NA, Millet EJ, Fredberg JJ (2003) Time scale and other invariants of integrative mechanical behaviour in living cells. Phys Rev E 68(041914):1–18

Guck J, Ananthakrishnan R, Mahmood H, Moon TJ, Cunningham C C, Käs J (2001) The optical stretcher: a novel laser tool to micromanipulate cells. Biophys J 81:767–784

Janmey PA (1998) The cytoskeleton and cell signaling: component localization and mechanical coupling. Physiol Rev 78:763–780

Janmey PA, Euteneuer U, Traub P, Schliwa M (1991) Viscoelastic properties of vimentin compared with other filamentous biopolymer networks. J Cell Biol 113:155–160

Kovacs M, Toth J, Hetényi C, Malnasi-Csizmadadia A, Sellers JR (2004) Mechanism of blebbistatin inhibition by myosin II. J Biol Chem 279:35557–35563

Kruse K, Joanny JF, Jülicher F, Prost J, Sekimoto K (2004) Asters, vortices and rotating spirals in active gels of polar filaments. Phys Rev Lett 92:078101-1; 078101-4

Lau AWC, Hoffmann BD, Davies A, Crocker JC, Lubensky TC (2003) Microrheology, stress fluctuations, and active behaviour of living cells. Phys Rev Lett 91(198101):1–4

Laurent V, Hénon S, Planus E, Fodil R, Balland M, Isabey D, Gallet F (2002) Assessment of mechanical properties of adherent living cells by bead micromanipulation: comparison of magnetic twisting cytometry vs optical tweezers. J Biomech Eng 124:408–421

Le Goff L, Amblard F, Furst EM (2002) Motor-driven dynamics in actin-myosin networks. Phys Rev Lett 88:018101-1; 018101-4

Lenormand G, Hénon S, Richert A, Siméon J, Gallet F (2001) Direct measurement of the area expansion and shear moduli of the human red blood cell membrane skeleton. Biophys J 81:43–58

Lenormand G, Millet E, Fabry B, Butler JP, Fredberg JJ (2004) Linearity and time-scale invariance of the creep function in living cells. J R Soc Lond Interface 1:91–97

Maksym GN, Fabry B, Butler JP, Navajas D, Tschumberlin D J, Laporte JD, Fredberg JJ (2000) Mechanical properties of cultured human airway smooth muscle cells from 0.05 to 0.4 Hz. J Appl Physiol 89:1619–1632

Palmer A, Mason TG, Xu J, Kuo SC, Wirtz D (1999) Diffusing wave spectroscopy microrheology of actin filament networks. Biophys J 76:1063–1071

Petersen NO, McConnaughey WB, Elson EL (1982) Dependance of locally measured cellular deformability on position on the cell, temparature and cytochalasin D. Proc Natl Acad Sci USA 79:5327–5331

Puig-de-Morales M, Millet EJ, Fabry B, Navajas D, Wang N, Butler JP, Fredberg JJ (2004) Cytoskeletal mechanics in adherent human airway smooth muscle cells: probe specificity and scaling of protein-protein dynamics. Am J Physiol Cell Physiol 287:C643–C654

Rotsch C, Braet F, Wisse E, Radmacher M (1997) AFM imaging and elasticity measurements on living rat liver macrophages. Cell Biol Int 21:685–696

Sato M, Ohshima N, Nerem RM (1996) Viscoelastic properties of cultured porcine aortic endothelial cells exposed to shear stress. J Biomech 29:461–467

Sato M, Nagayama K, Kataoka N, Sasaki M, Hane K (2000) Local mechanical properties measured by atomic force microscopy for cultured bovine endothelial cells exposed to shear stress. J Biomech 33:127–135

Sollich P (1998) Rheological constitutive equation for a model of soft glassy materials. Phys Rev E 58:738–759

Sollich P, Lequeux F, Hébraud P, Cates ME (1997) Rheology of soft glassy materials. Phys Rev Lett 78:2020–2023

Straight AF, Cheug A, Limouze J, Chen I, Westwood NJ, Sellers JR, Mitchison TJ (2003) Dissecting temporal and spatial control of cytokinesis with a myosin II Inhibitor. Science 299:1743–1747

Thoumine O, Ott A (1997) Time scale dependent viscoelastic and contractile regimes in fibroblasts probed by microplate manipulation. J Cell Sci 110:2109–2116

Tseng Y, Kole TP, Wirtz D (2002) Micromechanical mapping of live cells by multiple-particle-tracking microrheology. Biophys J 83:3162–3176

Wilhelm C, Gazeau F, Bacri J-C (2003) Rotational magnetic endosome microrheology: viscoelastic architecture inside living cells. Phys Rev E 67:061908-1;061908-12

Yamada S, Wirtz D, Kuo SC (2000) Mechanics of living cells measured by laser tracking microrheology. Biophys J 78:1736–1747